Dalton Transactions

RSC Publishing

PAPER

View Article Online
View Journal | View Issue

Cite this: *Dalton Trans.*, 2013, **42**, 6131

Equilibrium and kinetic studies on complex formation and decomposition and the movement of Cu^{2+} metal ions within polytopic receptors†

Carmen Ester Castillo,[a] Jorge González-García,[b] José M. Llinares,[b] M. Angeles Máñez,[a] Hermas R. Jimenez,[b] Enrique García-España*[b] and Manuel G. Basallote*[a]

Potentiometric studies carried out on the interaction of two tritopic double-scorpiand receptors in which two equivalent 5-(2-aminoethyl)-2,5,8-triaza[9]-(2,6)-pyridinophane moieties are linked with 2,9-dimethylphenanthroline (**L1**) and 2,6-dimethylpyridine (**L2**) establish the formation of mono-, bi- and trinuclear Cu^{2+} complexes. The values of the stability constants and paramagnetic ^1H NMR studies permit one to infer the most likely coordination modes of the various complexes formed. Kinetic studies on complex formation and decomposition have also been carried out. Complex formation occurs with polyphasic kinetics for both receptors, although a significant difference is found between both ligands with respect to the relative values of the rate constants for the metal coordination steps and the structural reorganizations following them. Complex decomposition occurs with two separate kinetic steps, the first one being so fast that it occurs within the stopped-flow mixing time, whereas the second one is slow enough to allow kinetic studies using a conventional spectrophotometer. As a whole, the kinetic experiments also provide information about the movement of the metal ion within the receptors. The differences observed between the different receptors can be interpreted in terms of changes in the network of hydrogen bonds formed in the different species.

Received 22nd September 2012,
Accepted 28th January 2013

DOI: 10.1039/c3dt32220c

www.rsc.org/dalton

Introduction

Coordinated molecular reorganisations induced by chemical or physical input are central to life. For instance, Ca^{2+} induced conformational changes of the calmodulin family of proteins trigger the activity of different enzymes, ionic pumps and other proteins.[1] The rotational motion of flagella that permits the straight swimming of bacteria constitutes a beautiful example of a pH-driven molecular motion.[2]

In the last few years, research in polytopic receptors has focused on molecular recognition, enzyme mimicking, molecular devices and pharmaceutical chemistry.[3–5] Nevertheless, polytopic ligands having differentiated binding sites represent a landmark for investigating substrate reorganisation within receptor molecules.

An interesting characteristic in polytopic receptors featuring differentiated binding sites is the possibility for a given metal ion to move from one site to another depending on its intrinsic binding ability and on the protonation stage of the receptor.[6] In this respect, we have recently advanced results regarding the metal ion reorganisation occurring in mononuclear, binuclear and trinuclear Cu^{2+} complexes of ligand **L1** (see Chart 1).[7]

Such preliminary studies suggested that coordination was initially affecting the phenanthroline unit of the linker to move then towards the macrocyclic cavity; the final stage being the closure of the side-chain of the double scorpiand macrocycle. These molecular reorganisation studies of substrates guided kinetically in its intermediate stages but thermodynamically controlled in the final stage are scarce. In order to get further kinetic and thermodynamic information about these pH-driven metal ion reorganisations we have extended our studies to a related ligand containing pyridine as a linker (**L2** in Chart 1). Here, we analyse how the different length and chelation units of the linker influence the thermodynamic

[a]*Departamento de Ciencia de los Materiales e Ingeniería Metalúrgica, Facultad de Ciencias, Universidad de Cádiz, Polígono Rio San Pedro, s/n, Puerto Real, 11510 Cádiz, Spain. E-mail: manuel.basallote@uca.es*

[b]*Instituto de Ciencia Molecular, Departamentos de Química Inorgánica y Orgánica, Universidad de Valencia, C/Catedrático José Beltrán 2, 46980, Paterna, Valencia, Spain. E-mail: enrique.garcia-es@uv.es*

†Electronic supplementary information (ESI) available. See DOI: 10.1039/c3dt32220c

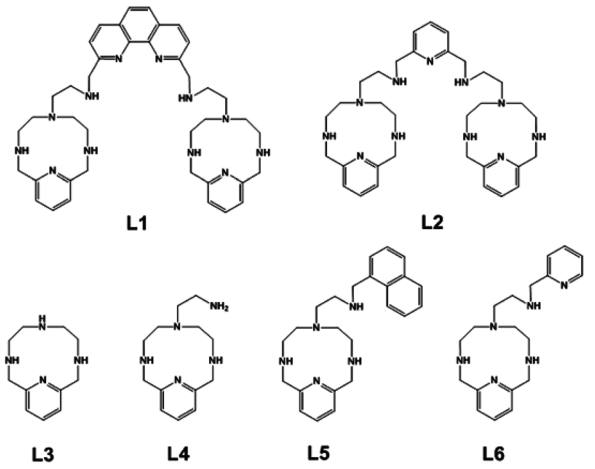

Chart 1

stability and the kinetics of formation and dissociation of the Cu^{2+} complexes.

Experimental section

L1, **L2**, **L3**, **L4**, **L5** and **L6** have been obtained by procedures described previously.[8–11] All the compounds were isolated as their hydrochloride or hydrobromide salts and gave satisfactory elemental microanalysis. All reagents were obtained from commercial sources.

EMF measurements

The potentiometric titrations were carried out at 298.1 ± 0.1 K using NaCl 0.15 M as a supporting electrolyte. The experimental procedure (burette, potentiometer, cell, stirrer, microcomputer, *etc.*) has been fully described elsewhere.[12] The acquisition of the emf data was performed with the computer program PASAT.[13] The reference electrode was an Ag/AgCl electrode in saturated KCl solution. The glass electrode was calibrated as a hydrogen-ion concentration probe by titration of previously standardized amounts of HCl with CO_2-free NaOH solutions and the equivalent point determined by Gran's method,[14] which gives the standard potential, $E^{\circ\prime}$, and the ionic product of water ($pK_w = 13.73(1)$). The computer program HYPERQUAD[15] was used to calculate the protonation and stability constants. The HYSS[16] program was used to obtain the distribution diagrams. The pH range investigated was 2.5–11.0 and the concentrations of Cu^{2+} and of the receptors ranged from 2×10^{-3} to 3×10^{-4} M with Cu^{2+} : L molar ratios varying from 3 : 1 to 1 : 1. For Cu^{2+} : L 3 : 1 molar ratio precipitation was observed above pH 8 for **L1** and above pH 6 for **L2**. Only the portions of the titration curves prior to precipitation were included in the refinement. The different titration curves for each system (6 for Cu^{2+}–**L1**, 728 experimental data points, and 4 for Cu^{2+}–**L2**, 285 experimental data points) were treated either as a single set or as separated curves without significant variations in the values of the stability constants.

Paramagnetic NMR spectroscopy

The paramagnetic NMR measurements were acquired on a Bruker Avance 400 spectrometer operating at 399.91 MHz. One-dimensional spectra were recorded in D_2O solvent with presaturation of the H_2O signal during part of the relaxation delay to eliminate the H_2O signal. Relaxation delay times of 50–400 ms, spectral widths of 30–75 kHz and acquisition times of 60–300 ms were used. NMR spectra were processed using exponential line-broadening weighting functions as apodization with values of 5–30 Hz. Chemical shifts were referenced to residual solvent protons of D_2O resonating at 4.76 ppm (298 K) relative to TMS. Sample concentrations for paramagnetic ^1H NMR were 2.5–3.0 mM in complexes. The longitudinal relaxation times of the hyperfine shifted resonances were determined using the inversion recovery pulse sequence (d_1-180°-τ-90°-acq, where d_1 is the relaxation delay and acq is the acquisition time), 15 values of τ were selected between 0.4 ms and 500 ms,[17] (d_1 + acq) values were at least five times the longest expected T_1 ranging from 100 to 800 ms, and the number of scans was 15 000. The T_1 values were calculated from the inversion-recovery equation. Transversal relaxation times were obtained measuring the line broadening of the isotropically shifted signals at half-height through the equation $T_2^{-1} = \pi\Delta\nu_{1/2}$.

Kinetic experiments

The kinetic experiments were carried out at 298.1 ± 0.1 K with both a Cary 50-BIO spectrophotometer and an Applied Photophysics SX17MV stopped-flow instrument provided with a PDA-1 diode array detector. The ionic strength was adjusted to 0.15 M for the formation studies and 1.0 M for the decomposition studies by adding the required amount of NaCl.

For kinetic studies on complex formation, a solution of the ligand whose pH had been previously adjusted with HCl and NaOH was mixed in the stopped-flow instrument with a solution of Cu^{2+} containing the amount of metal ion required to achieve 1 : 1, 2 : 1 or 3 : 1 Cu^{2+} : L molar ratios, although for **L2** the experiments at 3 : 1 Cu^{2+} : L ratio were unsuccessful because irreproducible results were obtained, probably because of precipitation at higher metal concentrations. The pH of the metal solution was adjusted to the same pH as the ligand solution. The kinetic experiments covered a pH range of *ca.* 2.5–5.5 and provided spectral changes with time that were analysed with either SPECFIT[18] or Pro-KII software.[19] At the low pH used the ligands are highly protonated and this makes the equilibrium constants for the formation of the outer-sphere complexes with Cu^{2+} small enough to make the rate of complex formation slow enough to be measured. The kinetic models used in each case are discussed in the Results and discussion section. As no buffers were used, there are large changes in proton concentration during complex formation, and so all the data corresponding to different experiments with different starting pH and molar ratios were finally fitted together using the Pro-KII software.[19] During this refinement, all the protonation equilibria revealed in the equilibrium

studies were taken into consideration with the equilibrium constants fixed at the values determined from potentiometric studies.

The kinetic work on complex decomposition was carried out under pseudo-first-order conditions of acid excess and the solutions contained Cu^{2+} and the corresponding ligand in 1 : 1, 2 : 1 and 3 : 1 molar ratios. To avoid possible complications with solutions containing mixtures of species, the equilibrium distribution curves were used to determine the pH values at which solutions containing Cu^{2+} and the ligand at a given molar ratio contain essentially a single species, and solutions prepared under these conditions were then mixed with an excess of acid. The spectral changes were registered using either a stopped-flow instrument or a conventional spectrophotometer, depending on the time scale. The pH was adjusted with NaOH and HCl solutions to values at which given $[CuH_xL]^{(2+x)+}$ and $[Cu_2H_xL]^{(4+x)+}$ complexes were the major species in solution. Data were analysed using the same software as for complex formation.

Table 1 Logarithms of the stability constants for the formation of mononuclear, binuclear and trinuclear complexes of Cu^{2+} : **L1** and **L2** calculated in 0.15 mol dm^{-3} NaCl at 298.1 ± 0.1 K

Reaction[a]	L1	L2
3H + Cu + L ⇄ CuH_3L	46.28(5)[b]	
2H + Cu + L ⇄ CuH_2L	39.25(6)	40.65(3)
H + Cu + L ⇄ CuHL	30.40(7)	33.07(5)
Cu + L ⇄ CuL	20.27(9)	23.8(1)
Cu + L + H_2O ⇄ CuL(OH) + H		
2H + 2Cu + L ⇄ Cu_2H_2L	47.74(9)	
H + 2Cu + L ⇄ Cu_2HL	45.03(7)	42.48(3)
2Cu + L ⇄ Cu_2L	39.31(9)	38.04(5)
2Cu + L + H_2O ⇄ $Cu_2L(OH)$ + H	28.84(9)	27.4(1)
3Cu + L ⇄ Cu_3L	44.19(1)	42.46(4)
CuH_2L + H ⇄ CuH_3L	7.02(6)	
CuHL + H ⇄ CuH_2L	8.85(3)	7.58(5)
CuL + H ⇄ CuHL	10.1(1)	9.27(5)
CuL + H_2O ⇄ CuL(OH) + H		
Cu_2LH + H ⇄ Cu_2H_2L	2.71(5)	
Cu_2L + H ⇄ Cu_2HL	5.72(4)	4.44(5)
CuL + Cu ⇄ Cu_2L	19.0(1)	14.24(5)
Cu_2L + H_2O ⇄ $Cu_2L(OH)$ + H	−10.46(6)	−10.64(5)
Cu_2L + Cu ⇄ Cu_3L	4.9(1)	4.42(5)

[a] Charges omitted. [b] Values in parentheses show standard deviation in the last significant figure.

Results and discussion

Interaction with Cu^{2+}

In order to check the thermodynamic properties of polytopic receptors with a biologically relevant metal ion, we have carried out potentiometric studies on the formation of Cu^{2+} complexes of **L1** and **L2**. The pH-metric titrations show formation of mono-, bi- and trinuclear species for both cases. The stoichiometries found for mono- and binuclear species are $[CuH_rL]^{(2+r)+}$ with r = 0–2 and $[Cu_2H_rL]^{(4+r)+}$ with r = −1 to 1 respectively, with additional triprotonated mononuclear and diprotonated binuclear species for **L1**. Furthermore, a trinuclear species was detected in solution for both receptors in the pH range covered in these measurements.

The stability constants for these complexes along with those found for the precursor **L3** and the derivatives **L4**, **L5** and **L6** (Chart 1) are collected in Table 1 and Table S1.†

Regarding the mononuclear complexes, the first aspect that deserves to be commented on is the significant difference in stability between the $[CuL]^{2+}$ complexes of both receptors. The stability constant for the formation of the $[Cu\mathbf{L2}]^{2+}$ complex is higher than that obtained for the Cu^{2+} complexes of the precursor receptor **L4** and comparable to the receptor **L6** (Table S1†). Taking into account these values and the crystal structures obtained for the Cu^{2+} complexes of **L4** and **L6**,[9,10] it can be suggested that the binding of the metal in the $[Cu\mathbf{L2}]^{2+}$ species is likely involving the four nitrogens of the macrocyclic unit, the secondary nitrogen of the tail and the pyridine nitrogen of the linker.

In the case of $[Cu\mathbf{L1}]^{2+}$, however, the metal ion would be pentacoordinated by the four nitrogen atoms of the macrocycle and the secondary nitrogen atom of the linker. In both systems, formation of binuclear complexes is observed above pH 4 for Cu^{2+} : L 2 : 1 molar ratio (Fig. 1 and S1†). The stepwise constants for the formation of the binuclear complexes (CuL^{2+} + Cu^{2+} ⇄ Cu_2L^{4+}; log K = 19.0 for **L1** and log K = 14.2 for **L2**, Table 1) show the absence of positive cooperativity in this process. Moreover, the much lower stepwise value obtained for the formation of $[Cu_2\mathbf{L2}]^{4+}$ indicates that the binding of the second metal ion will either involve a lower number of nitrogens than in **L1** or will require a molecular reorganisation of the coordination sphere, implying bond breaking and formation. The participation of the pyridine nitrogen of the tail in the binding of the metal ion has been ascertained in the crystal structure obtained for $[Cu\mathbf{L6}](ClO_4)_2$.[10]

The distribution diagrams show that the nuclearity of the species formed depends very much on the Cu^{2+}–receptor molar ratio (Fig. 1, S1–S3†). Trinuclear complexes are observed in the whole pH range above pH *ca.* 3 for 3 : 1 Cu^{2+}–receptor molar ratios for both systems. Although binuclear complexes have been reported in many systems consisting of two macrocycles linked by different alkyl or aryl bridges, to our knowledge, the number of systems in which trinuclear species has been evidenced is much more scarce.[20,21]

In order to get further information about the coordination mode of the binuclear Cu^{2+} complexes, paramagnetic ^{1}H NMR spectra have been performed for solutions containing $[Cu_2L]^{4+}$ complexes as major species.

In the last decade, paramagnetic ^{1}H NMR spectroscopy has been applied to the assignment of the isotropically shifted signals, as well as the characteristic properties of similar dinuclear copper complexes of pyridinophane[22] and terpyridinophane azamacrocyclic ligands.[23] In particular, these studies provide interesting information about the electronic structure and coordination geometry of the metal ions in solution.[24]

The paramagnetic ^{1}H NMR spectrum of the system Cu^{2+}–**L2** in a 2 : 1 molar ratio recorded in D_2O at pH = 7.8 shows, in the

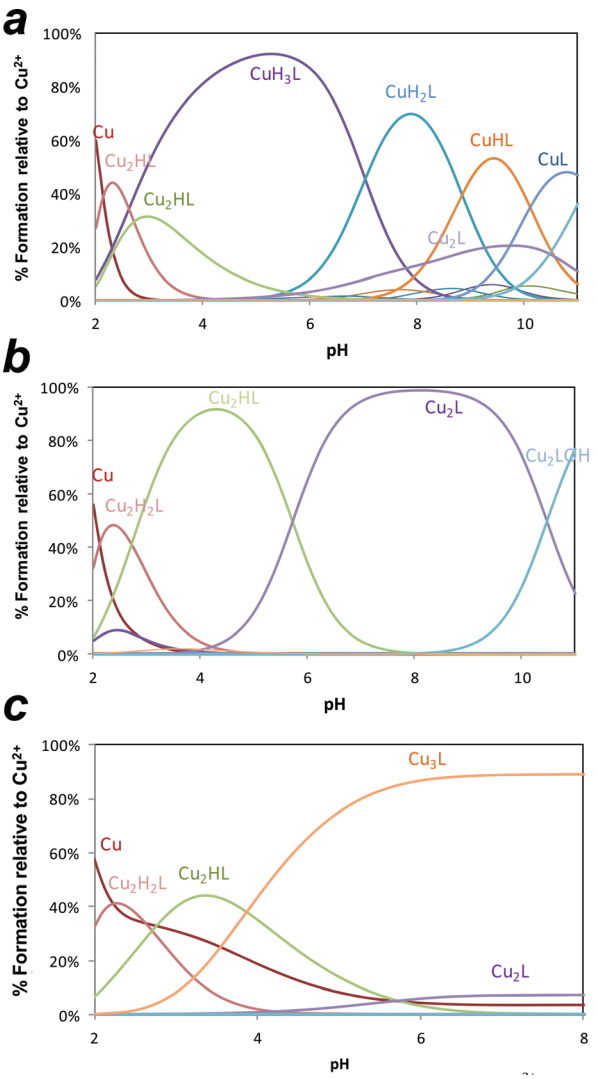

Fig. 1 Distribution diagrams of the species for the **L1**–Cu^{2+} systems as a function of pH in aqueous solution in 0.15 mol dm^{-3} at 298.1 K; [**L1**] = 1×10^{-3} M. (a) [Cu^{2+}] = 1×10^{-3} M, (b) [Cu^{2+}] = 2×10^{-3} M and (c) [Cu^{2+}] = 3×10^{-3} M. Charges omitted.

downfield region, three well resolved isotropically shifted signals (a′), (b′), (d′) and one non-resolved signal (c′). Chemical shift values, longitudinal relaxation time values (T_1), linewidths at half-height and assignments are reported in Table 2 and Scheme 1.

The NMR spectrum of $[Cu_2\mathbf{L2}]^{4+}$ presents two different groups of isotropically shifted signals, in the first group are set (a′) and (b′) whilst the second group gathers (c′) and (d′) signals.

The first type of signals (a′, b′) displays short T_1 values (<1 ms) and shows linewidths, measured at half-height, of around ~1000 Hz. The signals at 20.5 and 13.0 ppm integrating thirty-six protons are assigned on the basis of their large linewidths and short T_1 values, to the α-CH_2 protons closest to the copper sites (see Scheme 1). The second type of signals

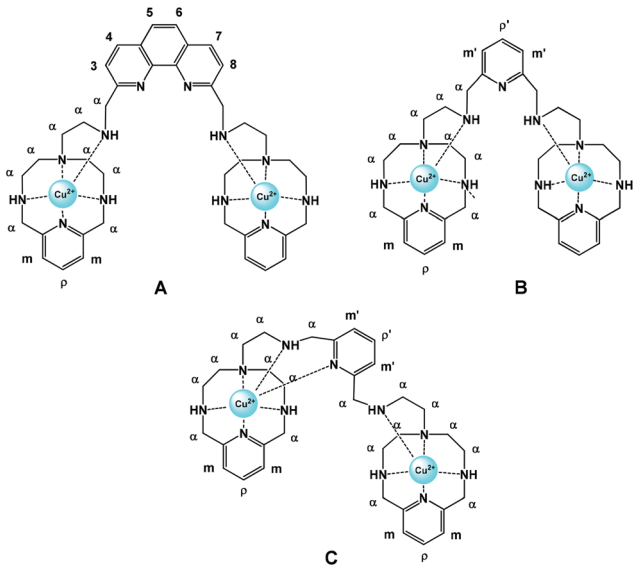

Scheme 1

Table 2 ^{1}H NMR hyperfine-shifted resonances of $[Cu_2\mathbf{L1}]^{4+}$ and $[Cu_2\mathbf{L2}]^{4+}$ complexes in D_2O at 298 K and pH = 7.8

System	Signal	δ (ppm)	No. of protons	Assignments	T^{re} dependence	T_1 (ms)	$\Delta\nu_{1/2}$ (Hz)	T_2[a] (ms)
$Cu_2\mathbf{L1}$	a	16.4			Curie	<1	840	0.38
	b	9.5			Indep.	2.7	~280	~1.1
	B[b]	10.3	36	α-CH_2	—	[c]	[c]	[c]
	c	8.8			Anti-Curie	2.3	[c]	[c]
	h	−1.9			Curie	<1	720	0.44
	e	8.4	6	$H_{m,p}$-Py	Anti-Curie	4.2	~128	~2.5
	d	8.7	4	$H_{3,4,7,8}$-Phen	Anti-Curie	5.2	[c]	[c]
	f	1.3	2	$H_{5,6}$-Phen	Anti-Curie	167.0	16	19.9
	g	1.1			Anti-Curie	62.9	14	22.7
$Cu_2\mathbf{L2}$	a′	20.5	36	α-CH_2	Curie	<1	1200	0.27
	b′	13.0			Curie	<1	840	0.38
	c′	10.2	9	$H_{m,p}$-Py	Anti-Curie	6.9	[c]	[c]
	d′	9.7		$H_{m',p'}$-Py	Anti-Curie	4.5	180	1.8

[a] Measured from the linewidth at half-height. [b] Measured at 313 K. [c] Overlap prevents measurement of this value.

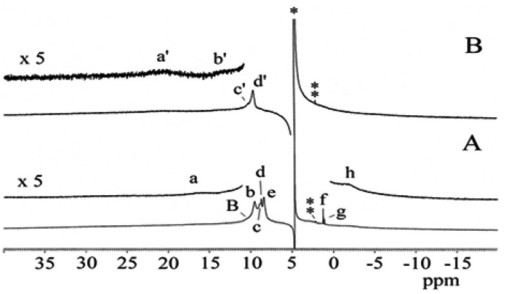

Fig. 2 400 MHz proton NMR spectra in D_2O at 298 K and pH = 7.7 of (A) $[Cu_2\mathbf{L1}]^{4+}$, (B) $[Cu_2\mathbf{L2}]^{4+}$. In the downfield and upfield regions, the intensity of the spectrum is multiplied by five. The asterisks mark the residual solvent and impurity signals (*, H_2O; **, HOD).

(c′, d′) that integrates nine protons and exhibits relatively short T_1 values (6.9 and 4.5 ms) can be assigned to the *meta* and *para* pyridine protons. The pattern of paramagnetic signals for the $[Cu_2\mathbf{L2}]^{4+}$ protons can be explained either by coordination mode **B** or by coordination mode **C**, both represented in Scheme 1. However, as above mentioned, the analysis of the stability constants seem to fit better with coordination mode **C**.

The ^{1}H NMR spectrum of the system Cu^{2+}–**L1** in a 2 : 1 molar ratio recorded in D_2O at pH = 7.8 shows, in the downfield region, three well resolved isotropically shifted signals (a), (b), (e) and three non-resolved signals (B), (c) and (d). In addition, three other signals (f–h) appear in the upfield region of the spectrum (see Table 2 and Fig. 2A). The NMR spectrum of $[Cu_2\mathbf{L1}]^{4+}$ presents important changes with respect to that of $[Cu_2\mathbf{L2}]^{4+}$. First, the number of isotropically shifted signals is higher in the spectrum of $[Cu_2\mathbf{L1}]^{4+}$ (see Fig. 2). Such an increase may be indicative of a more rigid and less symmetric structure that would lead to multiple structures for the isotropic shift resonances. Second, narrower linewidths and larger longitudinal relaxation times are observed for paramagnetic α-CH_2 signals. This behaviour can be interpreted as being due to the larger magnetic exchange of the phenanthroline group in the dicopper system in comparison with $[Cu_2\mathbf{L2}]^{4+}$. The group of signals corresponding to the pyridine protons ($H_{m,p}$-Py) of $[Cu_2\mathbf{L1}]^{4+}$ not only shows larger isotropically shifts but also narrower linewidths than those observed for $[Cu_2\mathbf{L2}]^{4+}$. All these results suggest pentacoordination for the two copper ions $[Cu_2\mathbf{L1}]^{4+}$ as depicted in Scheme 1A.

Variable temperature ^{1}H NMR spectra of $[Cu_2\mathbf{L1}]^{4+}$ and $[Cu_2\mathbf{L2}]^{4+}$ were registered from 283 to 323 K. Practically all observed isotropically shifted resonances follow an anti-Curie or temperature independent behaviour, except the isotropic shifts of resonances (a,h) and (a′,b′), corresponding to the α-CH_2 protons of macrocyclic ligands that show a Curie behaviour. These results agree with the existence of a magnetic interaction in coupled dinuclear copper(II) systems. Both dicopper systems show the existence of an antiferromagnetic interaction through the phenanthroline and pyridine bridges.

The constants for coordination of the third metal ion are quite lower ($Cu_2L^{4+} + Cu^{2+} \rightleftarrows Cu_3L^{6+}$; log K = 4.9) for **L1** than that for the Cu^{2+}-phen complex (log K = 7.4)[25] and much lower for **L2**, (log K = 4.42) than for the Cu^{2+}-2,6-bis(aminomethyl) pyridine complex (log K = 15.7). It has to be remarked that the precipitation occurring for both systems prevented to obtain any information about the likely formation of hydroxylated trinuclear species.

The difference in stability can be due to steric effects associated with the bulky linker units and to repulsion between the third metal ion and the highly positive binuclear complex. In addition, there is the possibility that coordination of the third Cu^{2+} occurs with structural reorganisation, so that the two previously coordinated metal centres are exclusively bound at the macrocyclic sites thus allowing for coordination of the entering Cu^{2+} at the phenanthroline and 2,6-bis(aminomethyl) pyridine sites respectively.

Moreover, paramagnetic experiments with solutions containing the $[Cu_3L]^{6+}$ complex were conducted. Unfortunately, precipitation of solutions containing **L2** prevented the study and only spectra for $[Cu_3\mathbf{L1}]^{6+}$ could be recorded.

The ^{1}H paramagnetic NMR spectrum of the complex $[Cu_3\mathbf{L1}]^{6+}$ in D_2O at pH = 7.2 shows a different pattern of chemical shifts than $[Cu_2\mathbf{L1}]^{4+}$, confirming the formation of the trinuclear complex.[7] The spectrum displays, in the downfield region, eleven well resolved isotropically shifted signals (a–d, h, i, k–n and A) and four non-resolved signals (e–g and j). Additionally, one upfield shifted signal (o) also appears in the spectrum (Fig. S4†). The hyperfine-shifted resonances, linewidths at half-height, longitudinal relaxation times values (T_1) and assignments are reported in Table 3 and Scheme 2. The NMR spectrum of $[Cu_3\mathbf{L1}]^{6+}$ presents some differences with the spectrum of $[Cu_2\mathbf{L1}]^{4+}$ previously studied. First, the isotropic shift of the α-CH_2 and pyridine–phenanthroline protons of the $[Cu_3\mathbf{L1}]^{6+}$ species is higher. Second, broader linewidths are found at least up to 1600 Hz and shorter longitudinal (T_1) and transversal (T_2) relaxation times. This behaviour can be interpreted as being due to the change in the coordination properties of the copper sites, and thereby in the magnetic properties of the metal ions in the trinuclear copper complex, see Scheme 2.

Moreover, the signals of the α-CH_2 protons of the $[Cu_3\mathbf{L1}]^{6+}$ move at least up to 40 ppm when compared to the spectrum of $[Cu_2\mathbf{L1}]^{4+}$ and the group of signals of phenanthroline protons ($H_{5,6}$-Phen) of the trinuclear system shows also linewidth broadening. These spectral features can be ascribed to a larger antiferromagnetic interaction between the three Cu^{2+} ions. Our results suggest for the $[Cu_3\mathbf{L1}]^{6+}$ two possible coordination modes, in the first one two copper ions would be pentacoordinated to the four nitrogens of the macrocyclic cavity and the nitrogen of the side arm while the third copper ion would be only coordinated to the phenanthroline ring completing its coordination sphere with solvent molecules. In the second coordination mode, the three copper ions would be four-coordinated; two of the copper ions would be bound by the nitrogens of the macrocyclic subunits while the third copper ion would be coordinated to the phenanthroline moiety and the two secondary amino groups of the arms (Scheme 2).

Table 3 ^{1}H NMR hyperfine-shifted resonances of $[Cu_3\mathbf{L1}]^{6+}$ complex in D_2O at 298 K and pH = 7.2

System	Signal	δ (ppm)	No. of protons	Assignment	T^{re} dependence	T_1 (ms)	$\Delta\nu_{1/2}$ (Hz)	T_2[a] (ms)
$Cu_3\mathbf{L1}$	*A*	56.2			Curie	<1	2570	0.12
	a	36.5			Curie	<1	914	0.35
	b	32.2			Curie	<1	686	0.46
	c	28.3			Curie	<1	800	0.40
	d	24.7	36	α-CH_2	Curie	<1	457	0.70
	e	20.4			Curie	<1	[b]	[b]
	f	18.6			Curie	<1	[b]	[b]
	g	16.6			Curie	<1	[b]	[b]
	o	−1.9			Curie	<1	578	0.55
	h	12.6	6		Anti-Curie	9.1	39	8.2
	l	8.7		H_p-py; $H_{4,5,6,7}$-phen	Anti-Curie	8.6	44	7.2
	m	7.6			Anti-Curie	8.0	53	6.0
	n	1.1			Anti-Curie	9.5	36	8.8
	i	11.6		H_m-py; $H_{3,8}$-phen	Anti-Curie	5.7	120	2.7
	j	10.3	6		Anti-Curie	[b]	[b]	[b]
	k	9.6			Anti-Curie	4.9	241	1.3

[a] Measured from the linewidth at half-height. [b] Overlap prevents measurement of this value.

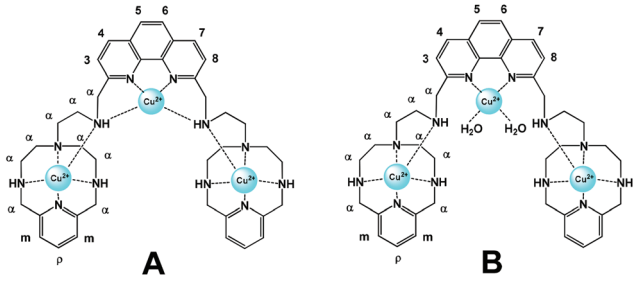

Scheme 2

However, the analysis of the stability constant values seems to fit better with the first proposed coordination mode (Scheme 2B).

Finally, although variable-temperature ^{1}H NMR studies of $[Cu_3\mathbf{L1}]^{6+}$ complex show Curie behaviour for most signals, there are a few signals exhibiting also anti-Curie behaviour, see Table 3. These results support a magnetically coupled trinuclear copper system.

Kinetics of formation of the Cu^{2+} complexes

The kinetics of complex formation between Cu_{aq}^{2+} and **L1–L2** was studied in moderately acidic media under non-pseudo first-order conditions, with the metal ion and the ligand in 1 : 1, 2 : 1 or 3 : 1 molar ratios. The experiments were carried out without adding any buffering agent because it has been shown that the addition of buffers often introduces some complications in this kind of kinetic studies.[9,19,26] As a consequence, the pH decreases during the reaction and the concentration of protons must be allowed to change during the refinement process, which is achieved by the simultaneous fit of all the kinetic data recorded under a variety of conditions with Pro-KII software.[19] According to the equilibrium results, the final reaction product is in general a mixture containing variable amounts of the different $[Cu_yH_xL]^{(2y+x)+}$ species, the nature and concentration of those species changing with starting pH, the nature of L and the Cu^{2+} : L molar ratio.

Despite the close similarity between **L1** and **L2**, the kinetic results for Cu^{2+} complexation with both ligands reveal a significantly different behaviour. Although in both cases the spectral changes denote polyphasic kinetics with pH-dependent observed rate constants, the kinetic models required for a satisfactory fit of the data are very different. The results for **L1** have been reported previously,[7] and the model used can be summarised indicating that the three Cu^{2+} ions are coordinated sequentially, the differences between the rate constants being large enough for allowing the processes to be observed in separate kinetic steps. Following the initial coordination of the metal ion, there are two reorganization steps that were interpreted as corresponding to the displacement of the metal ion from the phenanthroline linker to the macrocyclic site.

For the case of **L2**, the spectral changes require a model with three consecutive steps, the first one showing a first order dependence with respect to both the metal ion and the ligand, and the last two steps corresponding to reorganization processes with first-order rate constants. Preliminary fit of the individual data files revealed that the values of the rate constants change with the starting pH, all steps becoming faster at higher pH (see Fig. S5 in the ESI†). This finding indicates that all three resolved steps include acid–base pre-equilibria, which were considered a pre-requisite for all tested kinetic models. The numerical values derived for the rate constants of the three steps are similar for both the 1 : 1 and 2 : 1 Cu^{2+} : **L2** molar ratios. In addition, the spectra calculated for the intermediates formed in the different steps show an absorption band at the same wavelength for both molar ratios, but the molar absorptivities differ by a factor of 2 between the 1 : 1 and 2 : 1 experiments (see Fig. 3), thus suggesting that the same intermediates are formed in both sets of experiments, although at double concentration in the 2 : 1 experiments. A satisfactory fit is obtained when the data for both ratios are analysed simultaneously with the model in eqn (1)–(7). The

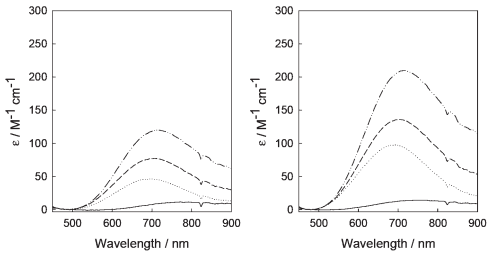

Fig. 3 Spectra calculated for the intermediates and the product in the reaction between Cu^{2+} and **L2** in 1 : 1 (left) and 2 : 1 (right) molar ratios using the kinetic model discussed in eqn (1)–(7). The four spectra in each figure correspond to Cu^{2+}, I_B, I_C and P, in order of increasing ε, although the spectra for I_B and I_C actually correspond to the spectra of equilibrium mixtures with I_{2B} and I_{2C}, respectively.

numerical values derived are $k_1 = 298 \pm 1\ M^{-1}\ s^{-1}$, $k_2 = 0.30 \pm 0.01\ s^{-1}$, $k_3 = 0.052 \pm 0.005\ s^{-1}$, $K_{BH} = (8 \pm 1) \times 10^3\ M^{-1}$, $K_{CH} = (2 \pm 1) \times 10^3\ M^{-1}$, with K_{H6L} fixed at the value derived from potentiometric data. As in the case of **L1**,[7] the reactive ligand species is $[H_5L2]^{5+}$. Because of precipitation no data could be obtained for the formation of trinuclear complexes.

The model used implies that complex formation occurs in three pH-dependent kinetic steps and that formation of the binuclear species occurs with statistically controlled kinetics,[9,19,26] *i.e.* coordination of both metal ions takes place in two consecutive processes with rate constants in a 2 : 1 molar ratio, although for mathematical reasons only a single process with a rate constant corresponding to coordination of the second ion is required to fit the experimental data.[27] The observation of statistical kinetics for complexation with **L2** and not with **L1** can be considered surprising, especially because the equilibrium constants for the formation of the mono- and binuclear complexes are much more different for **L2** than for **L1**. However, it must be considered that complex formation occurs through a complex mechanism with several kinetic steps, which makes meaningless the comparison of rate and equilibrium constants.

$$H_5L^{5+} + H^+ \rightleftarrows H_6L^{6+}; \quad K_{H6L} \tag{1}$$

$$H_5L^{5+} + Cu^{2+} \rightarrow I_A + H^+; \quad 2k_1 \tag{2}$$

$$I_A + Cu^{2+} \rightarrow I_B + H^+; \quad k_1 \tag{3}$$

$$I_B \rightleftarrows I_{2B} + H^+; \quad 1/K_{BH} \tag{4}$$

$$I_{2B} \rightarrow I_C; \quad k_2 \tag{5}$$

$$I_C \rightleftarrows I_{2C} + H^+; \quad 1/K_{CH} \tag{6}$$

$$I_{2C} \rightarrow P; \quad k_3 \tag{7}$$

After this initial step, two consecutive reorganisation processes take place leading to the final product, $[Cu_2HL2]^{5+}$, at the final pH values reached in the experiments. The final spectrum is similar to that reported for the copper complex of **L3**,[9,10] which suggests that the Cu^{2+} ions in $[Cu_2HL2]^{5+}$ are coordinated to the macrocyclic cavities, and the observation of a statistically controlled formation process would indicate that both cavities behave as independent units during complexation.

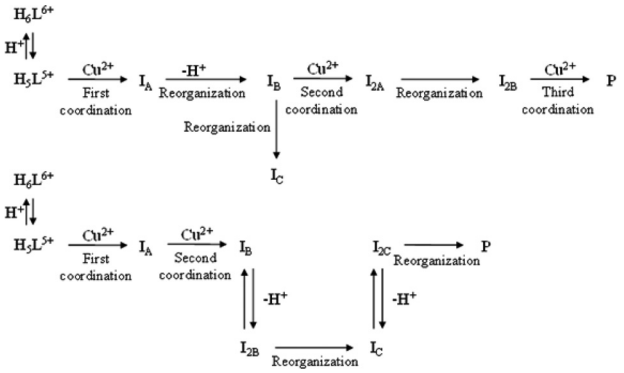

Fig. 4 Kinetic models used for fitting kinetic data for complex formation between Cu^{2+} and the receptors **L1** (up) and **L2** (down).

Table 4 Summary of kinetic data for complex formation between Cu^{2+} and the **L1–L6** receptors in moderately acidic solutions at 298.1 ± 0.1 K

Ligand	Reacting species	k_{L+Cu} ($M^{-1}\ s^{-1}$)	k_{CuL+Cu} ($M^{-1}\ s^{-1}$)
L1[a]	H_5L1^{5+}	1.27×10^4	3.80×10^2
L2[b]	H_5L2^{5+}	5.96×10^2	2.98×10^2
L3[c]	H_2L3^{2+}	1.1×10^2	—
L4[c]	H_3L4^{3+}	0.18	—
L5[c]	H_3L5^{3+}	0.36	—
L6[d]	H_3L6^{3+}	6.70×10^3	—

[a] Ref. 7. [b] This work. [c] Ref. 9. [d] Ref. 10.

Fig. 4 compares the kinetic models used for **L1** and **L2**, which include in both cases steps involving metal coordination and reorganisations. The two paths correspond to the two situations that arise for **L1** (upper path) and **L2** (lower path) depending on the relative values of the rate constants. For the case of **L1**,[7] the second Cu^{2+} is coordinated at a much slower rate than the first one ($k_1 = 1.27 \times 10^4\ M^{-1}\ s^{-1}$ and $k_2 = 3.80 \times 10^2\ M^{-1}\ s^{-1}$), and reorganizations following coordination of the first metal can be resolved because they are faster than the second coordination. The situation is different for **L2** because $k_1 = 2k_2$ and both coordination steps occur at close rates before the reorganisation processes. Thus, the major difference between both receptors derives from the occurrence of statistical kinetics for **L2** and deviations from it for **L1**. As statistical kinetics requires that the ligand is flexible enough to undergo rapidly all the structural changes required for coordination of the two metal ions,[28] it appears that the different rigidity introduced by the pyridine and phenanthroline linkers is the origin of the different kinetic behaviour observed for complex formation with both ligands.

Table 4 summarizes kinetic data for metal coordination to the **L1–L6** receptors. The species leading to complex formation in acidic solutions changes from $[H_2L]^{2+}$ to $[H_5L]^{5+}$, depending on the ligand. The data indicate that the complexation rate is not determined by the ligand charge but by the protonation

pattern and the network of hydrogen bonds in each protonated species. Actually, the fastest reaction occurs with $[H_5\mathbf{L1}]^{5+}$ despite the unfavorable charge effect because the phen site is accessible; *i.e.* it is unprotonated and not hydrogen-bonded.

Kinetics of acid-promoted decomposition of the Cu^{2+} complexes

According to the species distribution diagrams (Fig. 1 and S1†), the addition of an excess of acid to solutions of the metal complexes results in decomposition with release of Cu_{aq}^{2+} and protonated ligand (eqn (8)), and the kinetics of decomposition can be studied by monitoring the disappearance of the absorption band of the complex.[7,9,10,29]

$$[Cu_nH_mL]^{2+} + H_{exc}{}^{+} \rightarrow nCu^{2+} + (H_xL)^{x+} \quad (8)$$

A common feature in the decomposition of all the species studied for the **L1–L2** ligands is the existence of a rapid step within the mixing time of the stopped-flow instrument (*ca.* 1.7 ms), which is signalled by a shift of the absorption band upon acid addition. In a later process, the band disappears with very slow kinetics, *i.e.* complex decomposition occurs with biphasic kinetics, although the first step is too fast for its rate constant (k_{1obs}) to be measured. The spectral changes for decomposition of the intermediate are fitted satisfactorily by a single exponential (k_{2obs}).

For the **L1** complexes, the rapid step involves a shift to 750 nm of the absorption band observed at 640, 647 or 710 nm for the mono-, di- and trinuclear species, thus showing that the same intermediate is formed in all cases. The rate constants k_{2obs} for disappearance of the intermediate with a band at 750 nm show a linear dependence with respect to the acid concentration (Fig. 5), and the fit of all the data by eqn (9) yields $a = (1.8 \pm 0.7) \times 10^{-4}$ s^{-1} and $b = (3.2 \pm 0.1) \times 10^{-3}$ M^{-1} s^{-1}.

$$k_{2obs} = a + b[H^+] \quad (9)$$

$$k_{2obs} = c + d[H^+]^2 \quad (10)$$

In the case of **L2**, the step occurring within the stopped-flow mixing time involves a shift of the absorption band from 690 to 730 nm (Fig. 6), and the k_{2obs} values show a second order dependence with respect to the acid (eqn (10)), a kinetics reported previously for related metal–polyamine complexes.[9,30] Again, the whole set of data for different species can be fitted together and yield $c = (1.4 \pm 0.6) \times 10^{-4}$ s^{-1} and $d = (3.1 \pm 0.2) \times 10^{-3}$ M^{-2} s^{-1}.

The decomposition kinetics of the Cu^{2+} complexes with **L1** and **L2** is not very different from that observed for complexes with the related **L4–L6** receptors (see Table 5). In most of these cases complex decomposition starts with a rapid process that occurs within the stopped-flow mixing time and yields an intermediate that decomposes in a slower step with either a first or a second order dependence with respect to the proton concentration. This initial rapid step must involve protonation of the free amine groups and, eventually, dissociation of a Cu^{2+} ion and breaking of some Cu–N bonds. For complexes with the simpler **L4** and **L5** scorpiand-type ligands, the rapid step corresponds to protonation of the pendant arm and involves a shift of the band to 690 nm, the position observed for the **L3** complex, which lacks a side arm and decomposes in a single slow process.[9] Table 5 shows that only **L1** and **L2** form intermediates with absorption at 730–750 nm, which indicates that the intermediate formed with those ligands is different. In the case of **L1** it was proposed that the intermediate corresponds to a mononuclear complex with Cu^{2+} coordinated to the phen subunit,[26] but a similar interpretation is not possible for **L2** because Cu^{2+}–py complexes do not show an absorption band at *ca.* 730 nm.[31] Moreover, the band at 690 nm for $[CuH_2\mathbf{L2}]^{4+}$ and $[Cu_2\mathbf{L2}]^{4+}$coincides with that observed for the **L3** complex, which suggests that these complexes contain Cu^{2+} coordinated at the macrocyclic site/s of **L2**. According to the

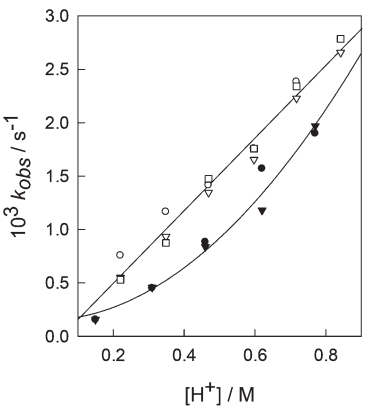

Fig. 5 Plot of the dependence on the acid concentration of the observed rate constant for the second kinetic step in the acid-promoted decomposition of the $[CuH_2L]^{4+}$ (filled circles) and $[Cu_2L]^{4+}$ (filled triangles) complexes ([NaCl] = 0.15 mol dm^{-3}, 298.1 K). The figure also includes data for the decomposition of the mono-, bi- and trinuclear species with **L1** (white symbols). The lines correspond to the best fit of the whole set of data for all the complex species with the same ligand.

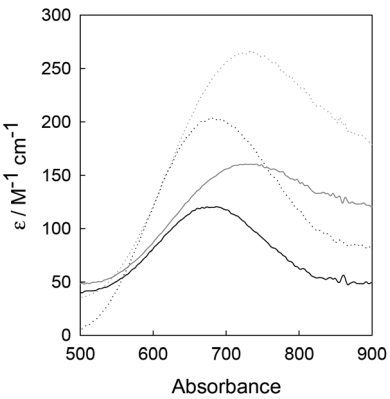

Fig. 6 Electronic spectra of complexes $[CuH_2\mathbf{L2}]^{4+}$ 6 × 10^{-4} M (continuous black line) and $[Cu_2\mathbf{L2}]^{4+}$ 6 × 10^{-4} M (dotted black line) and the first spectra obtained after mixing on the stopped-flow instrument with an excess of acid for $[CuH_2\mathbf{L2}]^{4+}$ (continuous grey line) and $[Cu_2\mathbf{L2}]^{4+}$ (dotted grey line).

Table 5 Summary of kinetic data for decomposition of the complexes formed between Cu^{2+} and the **L1–L6** receptors at 298.1 ± 0.1 K

Ligand	λ_{max}[a] (nm)	$[H^+]$ dependence	a or c[b] (s^{-1})	b (M^{-1} s^{-1}) or d[b] (M^{-2} s^{-1})
L1[c]	750	First order	1.8×10^{-4}	3.2×10^{-3}
L2[d]	730	Second order	1.4×10^{-4}	3.1×10^{-3}
L3[e]	695[g]	Second order	5.2×10^{-4}	1.16
L4[e]	690	First order	—	5.0×10^{-4}
L5[e]	690	First order	3×10^{-5}	3.9×10^{-4}
L6[f]	640[g]	First order	—	9.7×10^{-4}

[a] Absorption band of the intermediate formed within the stopped-flow mixing time. [b] Parameters a, b, c and d refer to eqn (9)–(10). [c] Ref. 7. [d] This work. [e] Ref. 9. [f] Ref. 10. [g] In this case there is no formation of any detectable intermediate and the complex decomposes in a single slow step.

behaviour observed for the **L4** and **L5** complexes one would expect a slow disappearance of the band at 690 nm, so that the observation of an additional rapid process with a shift of the band to 730 nm is unexpected. Participation of the linking pyridine cannot be invoked because a band at that wavelength has not been observed for **L6**, which contains pyridine in a similar arrangement,[10] or for a related ligand containing quinoline.[32] The species distribution curves indicate that the only stable species that can be an intermediate in $[CuH_2\mathbf{L2}]^{4+}$ and $[Cu_2\mathbf{L2}]^{4+}$ decomposition is $[Cu_2H\mathbf{L2}]^{5+}$, but formation of a binuclear species during the decomposition of the mononuclear complex is not reasonable and so it must be concluded that the intermediate is a metastable protonated species non-detectable by potentiometric studies. At this point, it can be pointed out that TD-DFT calculations on mononuclear Cu^{2+} complexes with tren-based ligands anticipate absorption bands at 710–770 nm for intermediates with trigonal bipyramidal (tbp) geometries and the ligand acting as a tri or tetradentate.[33]

Any of both dependences on the acid concentration can be rationalized on the basis of the mechanism usually proposed for the acid-promoted decomposition of polyamine complexes.[29,34] Complex decomposition is assumed to start with the initial formation of an intermediate $(CuL^{2+})^*$ in which there is elongation of the Cu–N that is going to be broken in the rate determining step, as indicated in eqn (11) for decomposition of a general CuL^{2+} complex. The next step is rate determining bond breaking, which can occur through two parallel pathways involving attacks by water and protons, respectively. The pathway involving water attack, eqn (12), is responsible for the a and c terms in eqn (9) and (10), whereas the pathway involving proton attack leads to the b and d terms. The difference between both equations is that a second order dependence on H^+ indicates that the rate determining step is shifted to the breaking of at least the second Cu–N bond (eqn (14)), whereas first order on H^+ is compatible with rate-determining attack by a single proton to cause dissociation of the first Cu–N bond, eqn (13).[9]

$$CuL^{2+} \rightleftarrows (CuL^{2+})^*; \quad k_1, k_{-1} \tag{11}$$

$$(CuL^{2+})^* + H_2O \rightarrow Cu^{2+} + H_xL^{x+}; \quad k_{H2O} \tag{12}$$

$$(CuL^{2+})^* + H^+ \rightarrow Cu(HL)^{3+}; \quad k_H \tag{13}$$

$$Cu(HL)^{3+} + H^+ \rightarrow Cu^{2+} + H_xL^{x+}; \quad k_{H2} \tag{14}$$

Conclusion

As stated in the Introduction, one of the major aims of the present work was to obtain additional information on the existence of well-defined pathways for the movement of metal ions within polytopic macrocyclic receptors. The present results, when taken together with those recently reported,[7] indicate that subtle changes in the structure of the receptor can lead to important changes in the kinetics of reaction. Thus, whereas for the phen-containing **L1** receptor the entry of the different metal ions occurs with significantly different rate constants and follows a well-defined pathway that goes from the linking phen to the macrocyclic cavities, the same is not true for the related py-containing **L2**. In the latter case, the macrocyclic subunits behave independently, thus indicating a passive role of the linking py in the process. It appears that the changes in the hydrogen-bond network associated with changing from phen to py as the linking sub-unit is large enough to cause such drastic kinetic changes. With regard to the exit of the metal ions, examined by studying the kinetics of complex decomposition, the results for the **L2** complexes indicate that the way that the metal ions follow for exiting from these receptors is not necessarily the same one used for entering.

Acknowledgements

Financial support by the Spanish MICINN and FEDER (Grants CTQ2009-14443-C02-01 and CTQ2009-14288-CO4-01), Consolider-Ingenio 2010 Program (Grant CSD2010-00065) and Generalitat Valenciana (PROMETEO 2011/008) is gratefully acknowledged. J. G. wants to thank the Spanish MICINN for a FPU fellowship.

Notes and references

1 T. R. Soderling and J. T. Stull, *Chem. Rev.*, 2001, **101**, 2341–2352.
2 M. Meister, S. R. Caplan and H. C. Berg, *Biophys. J.*, 1989, **55**, 905–914.
3 (*a*) J. M. Lehn, *Supramolecular Chemistry. Concepts and Perspectives*, VCH, Weinheim, 1995; (*b*) H. J. Schneider, *Principles and Methods in Supramolecular Chemistry*, John Wiley & Sons, Chichester, UK, 2000; (*c*) *Supramolecular Chemistry of Anions*, ed. A. Bianchi, K. Bowman-James and E. García-España, John Wiley & Sons, Chichester, UK, 1997;

(*d*) J. L. Sessler, P. A. Gale and W. S. Cho, *Anion Receptor Chemistry*, RSC Publishing, Cambridge, UK, 2006; (*e*) C. Caltagirone and P. A. Gale, *Chem. Soc. Rev.*, 2009, **38**, 520–563; (*f*) J. W. Steed, *Chem. Soc. Rev.*, 2009, **38**, 506–519; (*g*) S. Kubik, C. Reyheller and S. Stuwe, *J. Inclusion Phenom. Macrocyclic Chem.*, 2005, **52**, 137–187; (*h*) H. J. Schneider and A. K. Yatsimirsky, *Chem. Soc. Rev.*, 2008, **37**, 263–277; (*i*) *Anion Coordination Chemistry*, ed. K. Bowman-James, A. Bianchi and E. García-España, John Wiley & Sons, Chichester, UK, 2012.

4 (*a*) C. Bazzicalupi, A. Bencini, A. Bianchi, A. Danesi, C. Giorgi, C. Lodeiro, F. Pina, S. Santarelli and B. Valtancoli, *Chem. Commun.*, 2005, 2630–2632; (*b*) Q. X. Xiang, J. Zhang, P. Y. Liu, C. Q. Xia, Z. Y. Zhou, R. G. Xie and X. Q. Yu, *J. Inorg. Biochem.*, 2005, **99**, 1661–1669; (*c*) E. García-España, P. Gaviña, J. Latorre, C. Soriano and B. Verdejo, *J. Am. Chem. Soc.*, 2004, **126**, 5082–5083.

5 (*a*) S. K. Kim, D. H. Lee, J.-I. Hong and J. Yoon, *Acc. Chem. Res.*, 2009, **42**, 23–31; (*b*) S. Develay, R. Tripier, M. Le Baccon, V. Patinec, G. Serratrice and H. Handel, *Dalton Trans.*, 2006, 3418–3426; (*c*) S. Aoki, H. Kawatani, T. Goto, E. Kimura and M. Shiro, *J. Am. Chem. Soc.*, 2001, **123**, 1123–1132; (*d*) M. T. Albelda, J. C. Frias, E. García-España and S. V. Luis, *Org. Biomol. Chem.*, 2004, **2**, 816–820.

6 (*a*) L. Siegfried, C. N. McMahon, J. Baumeister, M. Neuburger, T. A. Kaden, S. Anandaram and C. G. Palivan, *Dalton Trans.*, 2007, 4797–4810; (*b*) M. P. Clares, S. Blasco, M. Inclan, L. Castillo, B. Verdejo, C. Soriano, A. Domenech, J. Latorre and E. García-España, *Chem. Commun.*, 2011, **47**, 5988–5990; (*c*) F. Durola, J. Lux and J.-P. Sauvage, *Chem.–Eur. J.*, 2009, **15**, 4124–4134; (*d*) J. González, R. Gavara, O. Gadea, S. Blasco, E. García-España and F. Pina, *Chem. Commun.*, 2012, **48**, 1994–1996.

7 C. E. Castillo, M. A. Mánez, J. González, J. M. Llinares, H. R. Jiménez, M. G. Basallote and E. García-España, *Chem. Commun.*, 2010, **46**, 6081–6083.

8 J. González, J. M. Llinares, R. Belda, J. Pitarch, C. Soriano, R. Tejero, B. Verdejo and E. García-España, *Org. Biomol. Chem.*, 2010, **8**, 2367–2376.

9 B. Verdejo, A. Ferrer, S. Blasco, C. E. Castillo, J. González, J. Latorre, M. A. Mañez, M. G. Basallote, C. Soriano and E. García-España, *Inorg. Chem.*, 2007, **46**(14), 5707–5719.

10 S. Blasco, B. Verdejo, M. P. Clares, C. E. Castillo, A. Algarra, J. Latorre, M. A. Mañez, M. G. Basallote, C. Soriano and E. García-España, *Inorg. Chem.*, 2010, **49**(15), 7016–7027.

11 (*a*) J. Costa and R. Delgado, *Inorg. Chem.*, 1993, **32**, 5257–5265; (*b*) V. Felix, J. Costa, R. Delgado, M. G. B. Drew, M. T. Duarte and C. J. Resende, *J. Chem. Soc., Dalton Trans.*, 2001, 1462–1471.

12 E. García-España, M. J. Ballester, F. Lloret, J. M. Moratal, J. Faus and A. Bianchi, *J. Chem. Soc., Dalton Trans.*, 1988, 101–104.

13 M. Fontanelli and M. Micheloni, *Proceedings of the I Spanish-Italian Congress on Thermodynamics of Metal Complexes*, Peñíscola, Castellón, 1990. Program for the automatic control of the microburette and the acquisition of the electromotive force readings.

14 (*a*) G. Gran, *Analyst*, 1952, **77**, 661–671; (*b*) F. J. Rossotti and H. Rossotti, *J. Chem. Educ.*, 1965, **42**, 375.

15 P. Gans, A. Sabatinni and A. Vacca, *Talanta*, 1996, **43**, 1739–1753.

16 P. Gans, *Programs to determine the distribution of species in multiequilibria systems from the stability constants and mass balance equations*, 2006.

17 R. L. Vold, J. S. Waugh, M. P. Klein and D. E. Phelps, *J. Chem. Phys.*, 1968, **48**, 3831–3832.

18 R. A. Binstead, B. Jung and A. D. Zuberbühler, *SPECFIT-32*, Spectrum Software Associates, Chappel Hill, 2000.

19 M. Maeder, Y. M. Neuhold, G. Puxty and P. King, *Phys. Chem. Chem. Phys.*, 2003, **5**(13), 2836–2841.

20 (*a*) E. Kimura, M. Kikuchi, H. Kitamura and T. Koike, *Chem.–Eur. J.*, 1999, **5**, 3113–3123; (*b*) G. Ambrosi, M. Formica, V. Fusi, L. Giorgi, E. Macedi, M. Micheloni, P. Paoli and P. Rossi, *Inorg. Chem.*, 2009, **48**, 10424–10434.

21 (*a*) M. Arca, A. Bencini, E. Berni, C. Caltagirone, F. A. Devillanova, F. Isaia, A. Garau, C. Giorgi, V. Lippolis, A. Perra, L. Tei and B. Valtancoli, *Inorg. Chem.*, 2003, **42**(21), 6929–6939; (*b*) A. Bencini, E. Berni, A. Bianchi, C. Giorgi, B. Valtanacoli, D. K. Chand and H. J. Schneider, *Dalton Trans.*, 2003, 793–800; (*c*) A. Bencini, S. Biagini, C. Giorgi, H. Handel, M. L. Baccon, P. Mariani, P. Paoletti, P. Paoli, P. Rossi, R. Tripier and B. Valtancoli, *Eur. J. Org. Chem.*, 2009, 5610–5621.

22 B. Verdejo, J. Aguilar, A. Doménech, C. Miranda, P. Navarro, H. R. Jiménez, C. Soriano and E. García-España, *Chem. Commun.*, 2005, 3086–3088.

23 B. Verdejo, S. Blasco, E. García-España, F. Lloret, P. Gaviña, C. Soriano, S. Tatay, H. R. Jiménez, A. Doménech and J. Latorre, *Dalton Trans.*, 2007, 4726–4737.

24 V. Clementi and C. Luchinat, *Acc. Chem. Res.*, 1998, **31**, 351–361.

25 R. L. Gustafson and A. E. Martell, *J. Am. Chem. Soc.*, 1959, **81**, 525–529.

26 (*a*) M. G. Basallote, J. Durán, M. J. Fernández-Trujillo, M. A. Máñez and B. Szpoganicz, *J. Chem. Soc., Dalton Trans.*, 1999, **7**, 1093–1100; (*b*) N. McCann, G. A. Lawrence, Y. M. Neuhold and M. Maeder, *Inorg. Chem.*, 2007, **46**, 4002–4009.

27 A. G. Algarra, M. J. Fernandez-Trujillo and M. G. Basallote, *Chem.–A Eur. J.*, 2012, **18**(16), 5036–5046.

28 M. G. Basallote, J. Duran, M. J. Fernandez-Trujillo and M. A. Manez, *J. Chem. Soc., Dalton Trans.: Inorg. Chem.*, 1999, **21**, 3817–3823.

29 (*a*) A. Mendoza, J. Aguilar, M. G. Basallote, L. Gil, J. C. Hernandez, M. A. Máñez, E. García-España, L. Ruiz-Ramirez, C. Soriano and B. Verdejo, *Chem. Commun.*, 2003, 3032–3033; (*b*) J. Aguilar, M. G. Basallote, L. Gil, J. C. Hernández, M. A. Máñez, E. García-España, C. Soriano and B. Verdejo, *Dalton Trans.*, 2004, 94–103.

30 (*a*) R. W. Hay, R. Bembi, W. T. Moodie and P. R. Norman, *J. Chem. Soc., Dalton Trans.*, 1982, 2131–2136;

(*b*) R. W. Hay, M. P. Pujari and F. McLaren, *Inorg. Chem.*, 1984, **23**, 3033–3035; (*c*) N. F. Curtis and S. R. Osvath, *Inorg. Chem.*, 1988, **27**, 305–310; (*d*) W. J. L. Hay, M. T. H. Tarafder and M. M. Hassan, *Polyhedron*, 1996, **15**, 725–732; (*e*) G. D. Santis, L. Fabbrizzi, A. Perotti, N. Sardone and A. Taglietti, *Inorg. Chem.*, 1997, **36**, 1998–2003.

31 (*a*) M. M. Tong and D. G. Brewer, *Can. J. Chem.*, 1971, **49**, 102–104; (*b*) R. V. Biagetti, W. G. Bottjer and H. M. Haendler, *Inorg. Chem.*, 1966, **5**(3), 379–382.

32 C. E. Castillo, M. A. Máñez, M. G. Basallote, M. P. Clares, S. Blasco and E. García-España, *Dalton Trans.*, 2012, **41**, 5617–5624.

33 A. Algarra, M. G. Basallote, C. E. Castillo, M. P. Clares, A. Ferrer, E. García-España, J. M. Llinares, M. A. Máñez and C. Soriano, *Inorg. Chem.*, 2009, **48**(3), 902–914.

34 (*a*) W.-J. L. Lan and C.-S. Chung, *J. Chem. Soc., Dalton Trans.*, 1994, 191–194; (*b*) L.-H. Chen and C.-S. Chung, *Inorg. Chem.*, 1989, **28**, 1402–1405.